

Investigation of Minimum Operating Temperatures for Cryogenic Wind Tunnels

Robert M. Hall* and Edward J. Ray*
NASA Langley Research Center, Hampton, Va.

Cryogenic wind tunnels should be operated at the lowest possible total temperature in order to maximize the advantages of cryogenic operation, such as increased Reynolds number and reduced drive power requirements. However, the minimum operating temperature is limited by effects of condensation on the flow. To determine when these effects occur, a 0.137-m NACA 0012-64 airfoil has been tested to extremely low temperatures at Mach numbers of 0.75, 0.85, and 0.95 for a total pressure range from 1.2 to 4.5 atm. No condensation effects were found to occur until total temperatures were below those associated with freestream saturation. Consequently, significant increases in Reynolds number capability were realized when compared to operations that avoid saturation over the airfoil. For the 0.85 and 0.95 Mach numbers, the increase in Reynolds number was at least 15% over the entire pressure range. The increase in Reynolds number was not influenced by total pressure during the 0.75 and 0.85 Mach tests, but there was some evidence of total pressure effects in the 0.95 Mach test.

Nomenclature

- C_p = pressure coefficient, $(p - p_\infty) / q_\infty$
 M = Mach number
 p = pressure
 q = dynamic pressure
 R = Reynolds number
 T = temperature
 x = linear dimension along airfoil chord line

Subscripts

- c = conditions based on airfoil chord, 0.137 m
 L = local conditions
 s = saturation curve conditions
 t = total conditions
 v = vapor conditions
 ∞ = freestream conditions

Introduction

THE Reynolds number capability of transonic wind tunnels has not kept pace with aircraft development during the past 20 years. In order to correct this situation, work has been underway both in the United States and in Europe to determine the type of wind tunnel best able to provide a high-Reynolds-number transonic environment. Following the NASA Langley Research Center development of the cryogenic concept,¹ the United States has decided to build a fan-driven, cryogenic, transonic tunnel at Langley. The construction of this national transonic facility will result in an order-of-magnitude increase in Reynolds number capability for transonic testing in this country.

In the Langley cryogenic wind-tunnel concept, the large increase in test Reynolds number is achieved by cooling the nitrogen test gas to extremely low temperatures. As the test gas temperature decreases for a given Mach number, the viscous force term in the expression for Reynolds number decreases markedly, while the inertial force term remains constant. Consequently, the Reynolds number is increasing while avoiding the adverse effects of increased inertial forces, such as larger model, support, and balance loads. As shown in

Fig. 1, the colder the test gas becomes, the greater the rate of increase in Reynolds number. Real-gas effects, however, potentially place a lower temperature limit on cryogenic tunnel operation. Since the national transonic facility will use both cryogenic temperatures and high pressures to achieve its high Reynolds number, it is important to know the lower temperature limit of tunnel operation in order to realize the most benefit from the cryogenic temperatures and therefore minimize the total pressure required for a given test Reynolds number.

The first category of real-gas effects which could limit low-temperature testing are possible differences between the real-gas behavior of the low-temperature nitrogen gas seen by the model in the tunnel and the nearly ideal-gas behavior of the air seen by the flying aircraft. These possible differences have been investigated by Adcock and coworkers,² and were shown to be insignificant for low-temperature testing at pressures below 5 atm. Their conclusions were based on both analytical work and on experimental data taken in the operational 1/3-m transonic cryogenic tunnel at Langley. Thus, the lower limit for valid, cryogenic testing is most probably fixed by the second category of real-gas effects—condensation effects.

The purpose of the present investigation is to experimentally determine the total temperatures corresponding to the onset of condensation effects over an airfoil for a range of pressures and freestream Mach numbers.

Prerequisites for Condensation

Condensation effects occur when there is enough condensate in the flow to alter some flow property noticeably, such as pressure, temperature, or sound speed. In order for condensation to occur, however, the static pressure and temperature of the gas must be on the lower temperature side of the saturation curve for nitrogen. When this does occur, the flow is said to be supersaturated.

In order to determine how much of the flow in the wind-tunnel circuit is supersaturated, it is necessary to compare the total temperature of the test to the total temperatures associated with three different stages of saturation possible in a wind-tunnel experiment. The first is the total temperature associated with saturated flow in the maximum local Mach number region, and hence minimum temperature region, over the model. Any test with a total temperature below this value will have supersaturated flow over the model. The second total temperature of interest is that associated with a saturated

Presented as Paper 76-89 at the AIAA 14th Aerospace Sciences Meeting, Washington, D.C., Jan. 26-28, 1976; submitted Feb. 2, 1976; revision received Jan. 24, 1977.

Index categories: Multiphase Flows; Testing, Flight and Ground; Research Facilities and Instrumentation.

*Aeronautical Research Scientist, Fluid Dynamics Branch, Subsonic-Transonic Aerodynamics Division. Member AIAA.

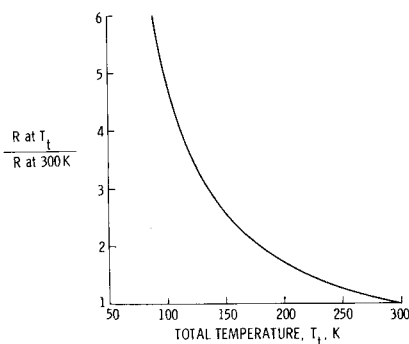


Fig. 1 Ratio of Reynolds number at T_t to Reynolds number at $T_t = 300$ K as a function of total temperature. Example shown was made for a total pressure of 5 atm and a freestream Mach number of 0.85.

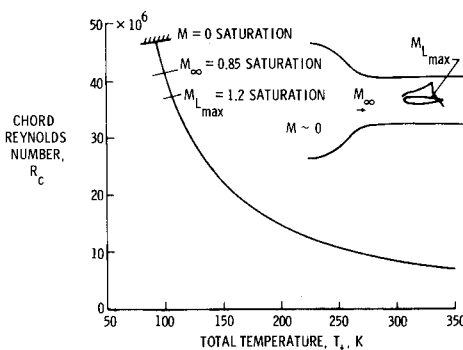


Fig. 2 Variation of chord Reynolds number with total temperature showing the values of chord Reynolds number at local, freestream, and reservoir saturation total temperatures. Example shown was made for the 0.137-m NACA 0012-64 airfoil with a total pressure 4.5 atm and a freestream Mach number of 0.85.

freestream. Flow with a total temperature below the freestream saturation total temperature will be supersaturated in the test section, as well as over the model. The third total temperature is that associated with the saturation temperature of the reservoir section of the wind tunnel. This last temperature represents the operational limit of the 1/3-m tunnel, because the tunnel is cooled by direct injection of liquid nitrogen. If the total conditions are saturated, the injected liquid will not be able to evaporate and will fill the tunnel with liquid. An example of the three total temperatures at which the maximum local Mach region, the freestream, and the reservoir become saturated is shown in Fig. 2; it is a plot of chord Reynolds number vs total temperature for the airfoil used in the present experiments.

Tests

As seen in Fig. 2, the Reynolds number is increasing rapidly at the lower temperatures associated with saturation. Consequently, if the tunnel total temperature could be lowered below local saturation without condensation effects, a significant increase in Reynolds number could be realized. Fortunately, testing with supersaturated flow does not necessarily give rise to the formation of liquid droplets, or condensate, under the dynamic conditions of wind-tunnel testing. There are a variety of factors that affect the presence and magnitude of condensation, such as the degree of supersaturation, the availability of foreign impurities, and the length of time for which the flow is supersaturated.

In order to determine the total temperature at which effects do occur and to investigate the influence of total pressure and freestream Mach number on the onset of condensation effects, an experimental program was undertaken. A 0.137-m NACA 0012-64 airfoil was mounted in the Langley 1/3-m transonic cryogenic tunnel and tested at freestream Mach

numbers of 0.75, 0.85, and 0.95 over a total pressure range of 1.2 to 5.0 atm. The data from the 0.85 Mach number test were reported earlier,³ and will be presented only in summary form in the section "Increased Reynolds Number Capability."

Experimental Apparatus

Tunnel

The Langley 1/3-m transonic cryogenic tunnel is a continuous flow, fan-driven tunnel, which uses nitrogen as a test gas and is cooled by injecting liquid nitrogen directly into the stream. Variation of the rate of liquid nitrogen injection provides a total temperature range from nearly 77 to 350 K, while the total pressure can be varied from 1.2 to 5 atm. The combined low temperature and high pressure can produce a Reynolds number of over 330 million/m (100 million/ft). Some of the design features and operational characteristics of the 1/3-m tunnel have been reported by Kilgore.⁴

Airfoil and Installation

A 0.137-m NACA 0012-64 airfoil was used for these tests. Starting at the leading edge, the airfoil had 20 pressure orifices spaced at 5% chord intervals on both the top and bottom surfaces. For the tests at Mach numbers of 0.75 and 0.95, a rearward-facing orifice was added to the trailing edge of the airfoil. The airfoil was installed between flats in the octagonal test section, with the leading edge 0.62 m from the beginning of the test section. The angle of attack of the airfoil was zero for all tests.

Data Acquisition and Error Discussion

The pressures over the airfoil were measured by using a differential pressure transducer and a scanning valve system. After the transducer output for all of the airfoil orifices was recorded, the tunnel parameters were recorded. The total time to acquire all of the information for a complete pressure distribution was 50 sec.

The uncertainty in the pressure transducer measurements was 0.5% of full scale. For the tests at a Mach number of 0.85, this uncertainty was 0.0085 atm, whereas for the tests at Mach numbers of 0.75 and 0.95, the uncertainty was 0.0170 atm. There was no significant error introduced by either the signal conditioning or the data acquisition systems. However, during the 50-sec acquisition period, the tunnel conditions were observed to fluctuate by the following amounts: Mach number, ± 0.003 ; total temperature, ± 0.5 K; and total pressure, ± 0.02 atm.

Results

The operating temperatures at which condensation effects first occurred in the flow about the NACA 0012-64 airfoil were determined for total pressures from 1.2 to 4.5 atm with freestream Mach numbers of 0.75 and 0.95. For each Mach number, a series of figures will be presented showing the total conditions sampled, the effects of condensation on the pressure distribution over the airfoil, and the experimentally determined temperature for the onset of condensation effects as a function of total pressure.

In some of the pressure distributions that will be presented, not all of the orifice pressures are shown. At various times during the test program, pressure leaks occurred in the tubing from the airfoil to the pressure gage. The values for the leaking orifices have not been plotted.

$M_\infty = 0.75$ Test

For this freestream Mach number, the maximum local Mach number over the airfoil was 0.93. The three total temperatures corresponding to local, freestream, and reservoir saturation are shown as a function of total pressure in Fig. 3. This figure also shows total pressure and temperature conditions representative of those sampled during

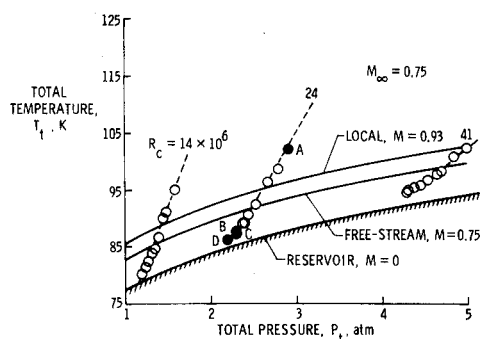


Fig. 3 Total temperatures corresponding to local, freestream, and reservoir saturation as a function of total pressure for a freestream Mach number of 0.75. Conditions sampled are shown along each path of constant chord Reynolds number.

the investigation. The conditions sampled were chosen from three different paths of constant chord Reynolds number. Since both Reynolds number and Mach number were constant along each path, the warmest temperature distribution serves as a standard for visual comparison with the lower temperature distributions. Any visually detected differences between the standard distribution and a lower temperature distribution are attributed to condensation effects. Because the warmest distributions for the $R_c = 14$ and 24 million path are clearly at a temperature above local saturation, there can be no effect of condensation in these standards used for comparison. For the $R_c = 41$ million path, the temperature of the standard is just below the local saturation temperature for that pressure. However, no condensation effects are expected in this standard distribution for two reasons. First, as will be seen along the lower Reynolds number paths, effects normally occur at much colder temperatures. Therefore, it is unlikely that condensation would occur so much sooner for the higher pressure. Second, no change in the pressure distribution along the $R_c = 41$ million path is detected as the temperature is reduced. If condensation effects were already present in the standard distribution, they would be expected to become progressively worse as the temperature was reduced further. The reason a warmer distribution was not used for the $R_c = 41$ million path, as well as for some paths in the $M_\infty = 0.85$ test, is that the tunnel total pressure limit is 5 atm. In order to increase the total temperature while maintaining a constant R_c , a total pressure greater than 5 atm would be required.

Typical results for this Mach number test can be summarized by looking at the $R_c = 24$ million path. As shown in Fig. 3, four total conditions have been labelled A, B, C, and D. The pressure distribution taken at total condition A serves as an unaffected, standard distribution with which to compare the lower temperature distributions that may be affected by condensation. The pressure distribution taken at point B was found to be the lowest temperature distribution that agrees with the standard taken at point A. The distribution taken at point C shows the first sign of effects, and is superimposed with the reference distribution in Fig. 4. Although the agreement shown in Fig. 4 is relatively good between the two distributions, there is a positive shift in the point C pressure distribution at and around the 50% chord position. In order to contrast the magnitude of this shift in the pressure coefficient, the shift in pressure coefficient that would result from a change in an orifice pressure of $p_\infty/100$ is shown in the upper left corner of Fig. 4. Also shown in the upper left corner is the uncertainty in pressure coefficient due to the stated accuracy of the pressure transducer. As seen in comparison, the condensation effects that are first seen in the distribution at point C are not large. Point D represents the lowest temperature distribution taken along this path of constant chord Reynolds number. The differences between the distribution at point D and point A, although not shown, are of the same magnitude as those in Fig. 4.

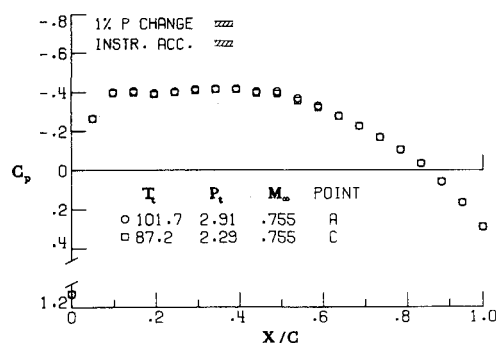


Fig. 4 Pressure distribution comparison showing effects of condensation. Point C is 3.4 K below freestream saturation.

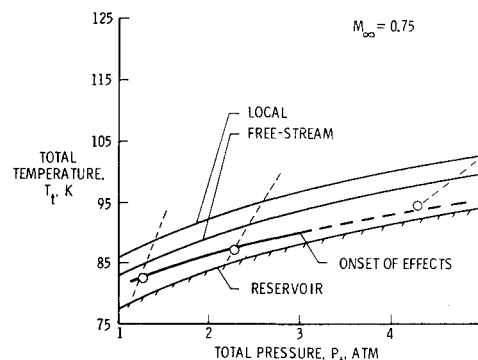


Fig. 5 Experimental curve for the onset of condensation effects as a function of total pressure. Freestream Mach number is 0.75.

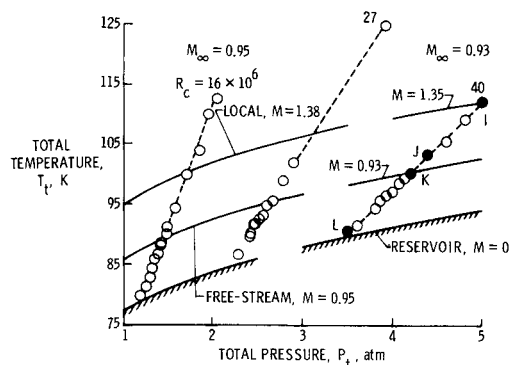


Fig. 6 Total temperatures corresponding to local, freestream, and reservoir saturation as a function of total pressure for freestream Mach numbers of 0.95 and 0.93. Conditions sampled are shown along each path of constant chord Reynolds number.

A graph of the total temperatures at which the onset of condensation effects were first detected is shown in Fig. 5. The points plotted represent the total temperature and pressure at which the first visually detected differences in pressure distribution were seen along each path of constant chord Reynolds number. For example, point C was plotted for the $R_c = 24$ million path. Along the $R_c = 41$ million path, however, no effects were detected, and so the onset curve is drawn below the lowest total temperature condition sampled.

$M_\infty = 0.95$ Test

Testing was done at $M_\infty = 0.95$ for two constant chord Reynolds number paths at lower pressures, but it was not possible to take high-pressure current data at $M_\infty = 0.95$ without exceeding the electrical current limit of the tunnel drive motor. However, $M_\infty = 0.93$ was attainable at the high pressures. Thus, Fig. 6 shows the saturation stages for both $M_\infty = 0.95$ and 0.93. The respective maximum local Mach

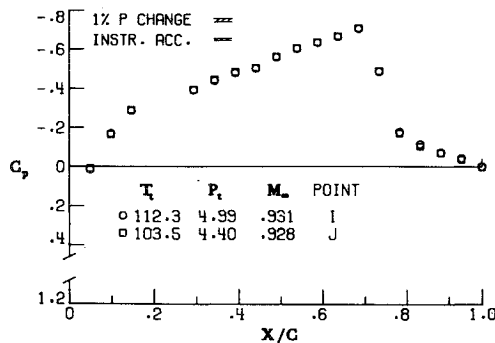


Fig. 7 Pressure distribution comparison showing no effects of condensation. Point J is 2.5 K above freestream saturation.

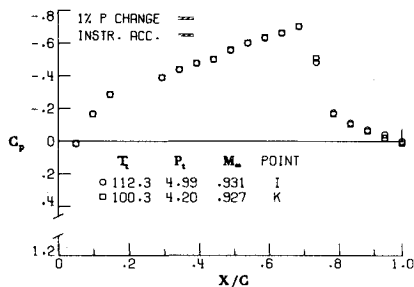


Fig. 8 Pressure distribution comparison showing effects of condensation. Point K is 0.1 K below freestream saturation.

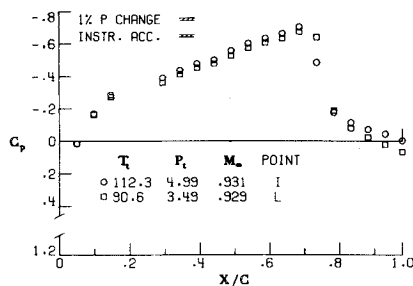


Fig. 9 Pressure distribution comparison showing effects of condensation. Point L is 7.6 K below freestream saturation.

numbers are 1.38 and 1.35. As shown in Fig. 6, three different R_c paths were investigated.

The points I, J, K, and L from Fig. 6 will be shown as typical comparisons for either the $M_\infty = 0.93$ or 0.95 paths. No effects are seen in the pressure distribution from point J, which is compared to the standard, point I, in Fig. 7. Point K shows the first signs of effects in Fig. 8. The differences between point K and the standard are quite different than in the lower M_∞ cases. Specifically, the differences occur at the shock and in the separated flow region behind the shock. The shock begins to move aft, while at the same time the pressure coefficient behind the shock is becoming more positive, which implies better recovery. These differences appear to be more complex than the differences one might expect from a shift in test Mach number. Under unsaturated conditions the shock moves aft and there is less pressure recovery when the Mach number increases. The unusual behavior of the shock and separated region is seen more clearly in Fig. 9, which compares the lowest temperature distribution point L, to the standard distribution, point I.

The graph showing the onset of condensation effects as a function of total pressure is presented in Fig. 10. The points plotted represent the total temperature and pressure at which the first visually detected differences in pressure distribution were seen along each R_c path.

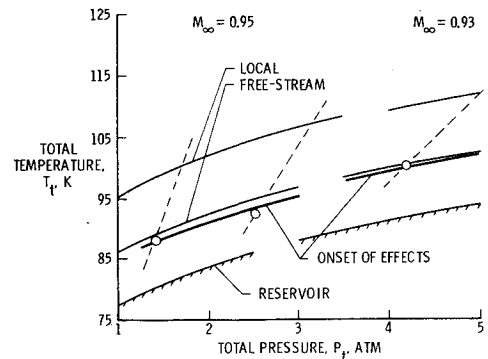


Fig. 10 Experimental curve for the onset of condensation effects as a function of total pressure. Freestream Mach numbers are 0.95 and 0.93.

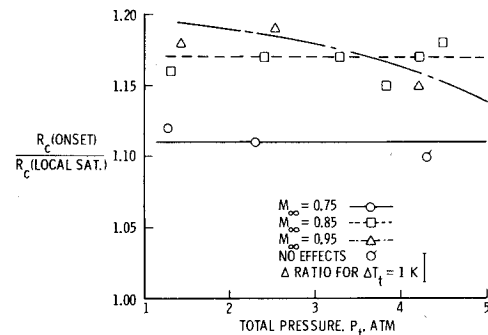


Fig. 11 Ratio of chord Reynolds number at onset of condensation effects to chord Reynolds number associated with local saturation, as a function of total pressure. (Flagged symbol represents the $R_c = 41$ million path in 0.75 Mach test, where no effects were observed.)

Increased Reynolds Number Capability

Before any condensation effects were observed, significant increases in Reynolds number for a given total pressure were realized by testing with supersaturated flow. A graph of the ratio of Reynolds number realized at the temperature corresponding to the onset of condensation effects over Reynolds number obtainable if local saturation is assumed to be the limiting condition is shown in Fig. 11. The results indicate that increases in Reynolds number ranging from 11% to about 18% appear to be obtainable, depending primarily on Mach number.

It is seen from Fig. 11 that the increase in Reynolds number is least (about 11%) at $M_\infty = 0.75$, even though the onset of condensation effects curve for $M_\infty = 0.75$ comes the closest to the reservoir saturation line. This is because lower freestream Mach numbers, such as 0.75, do not produce high local Mach numbers over the NACA 0012-64 airfoil at zero incidence, and therefore the difference between total temperatures associated with local and reservoir saturation is small. Since the increase in Reynolds number is a function of how many degrees below local saturation one may test before encountering effects, a large increase is not possible at lower Mach numbers. There do not appear to be any detrimental effects of increased total pressure for the $M_\infty = 0.75$ test.

The increase in Reynolds number at $M_\infty = 0.85$ is about 17% over the entire pressure range. Again, there do not appear to be noticeable pressure effects. However, for the $M_\infty = 0.95$ test, it does appear that there may be some reduction with increasing pressure of the 18% increase in Reynolds number realized at the lower pressures. Since this trend is based on only one data point, additional data are required to verify and properly describe this trend.

The error bar shown in Fig. 11 represents the difference in the ratio of Reynolds numbers that one would see if the total temperature for the onset of effects was in error by 1 K. An

uncertainty of 1 K is a reasonable estimate of the uncertainty in the onset temperature due to both instrument accuracy and the uncertainty in the visual comparison procedure for detecting differences.

Summary of Results

Total temperatures corresponding to the onset of condensation effects have been determined for flow over a 0.137-m NACA 0012-64 airfoil mounted in the Langley 1/3-m transonic cryogenic tunnel. Considerable supersaturation can develop before condensation effects become apparent for the 1.2- to 4.5-atm total pressure range investigated and the freestream Mach numbers of 0.75, 0.85, and 0.95. Consequently, significant increases in Reynolds number appear to be available by operating at tunnel temperatures below those associated with local saturation over the airfoil, but above those where effects first occur. For Mach numbers of 0.85 and 0.95, the Reynolds numbers at which effects occur are at least 15% greater than the Reynolds number achieved at local

saturation conditions for the same total pressures. The effects of pressure upon the increased Reynolds number capability do not appear to be detrimental for either the 0.75- or 0.85-Mach-number case. There may be some detrimental effects of higher pressure for the 0.95 Mach test, but more experimental work is required to clarify this pressure trend.

References

- ¹Polhamus, E. C., Kilgore, R. A., Adcock, J. B., and Ray, E. J., "The Langley Cryogenic High Reynolds Number Wind-Tunnel Program," *Astronautics & Aeronautics*, Vol. 12, Oct. 1974, pp. 30-40.
- ²Adcock, J. B., Kilgore, R. A., and Ray, E. J., "Cryogenic Nitrogen as a Transonic Wind-Tunnel Test Gas," AIAA Paper 75-143, Pasadena, Calif., Jan. 1975.
- ³Hall, R. M., "Preliminary Study of the Minimum Temperatures for Valid Testing in a Cryogenic Wind Tunnel," NASA TM X-72700, 1975.
- ⁴Kilgore, R. A., "Design Features and Operational Characteristics of the Langley Pilot Transonic Cryogenic Tunnel," NASA TM X-72012, 1974.

From the AIAA Progress in Astronautics and Aeronautics Series . . .

AEROACOUSTICS: JET AND COMBUSTION NOISE; DUCT ACOUSTICS—v. 37

Edited by Henry T. Nagamatsu, General Electric Research and Development Center; Jack V. O'Keefe, The Boeing Company; and Ira R. Schwartz, NASA Ames Research Center

A companion to Aeroacoustics: Fan, STOL, and Boundary Layer Noise; Sonic Boom; Aeroacoustic Instrumentation, volume 38 in the series.

This volume includes twenty-eight papers covering jet noise, combustion and core engine noise, and duct acoustics, with summaries of panel discussions. The papers on jet noise include theory and applications, jet noise formulation, sound distribution, acoustic radiation refraction, temperature effects, jets and suppressor characteristics, jets as acoustic shields, and acoustics of swirling jets.

Papers on combustion and core-generated noise cover both theory and practice, examining ducted combustion, open flames, and some early results of core noise studies.

Studies of duct acoustics discuss cross section variations and sheared flow, radiation in and from lined shear flow, helical flow interactions, emission from aircraft ducts, plane wave propagation in a variable area duct, nozzle wave propagation, mean flow in a lined duct, nonuniform waveguide propagation, flow noise in turbfans, annular duct phenomena, freestream turbulent acoustics, and vortex shedding in cavities.

541 pp., 6 x 9, illus. \$19.00 Mem. \$30.00 List

TO ORDER WRITE: Publications Dept., AIAA, 1290 Avenue of the Americas, New York, N. Y. 10019